CONF-811113--20

LA--UR-81-2713

TITLE: A PHASE-MODULATION INTERFEROMETER FOR ICF-TARGET CHARACTERIZATION

AUTHOR(S): David E. Cooper

SUBMITTED TO: 28th National Vacuum Symposium
Disneyland Hotel
Anaheim, California
November 3-6, 1981

MASTER

LOS ALAMOS SCIENTIFIC LABORATORY
Post Office Box 1663 Los Alamos, New Mexico 87545
An Affirmative Action/Equal Opportunity Employer

No. L36 R3
o. 2629

UNITED STATES
DEPARTMENT OF ENERGY
CONTRACT W-7405-ENG 36

A PHASE MODULATION INTERFEROMETER FOR ICF TARGET CHARACTERIZATION

David E. Cooper
University of California
Los Alamos National Laboratory
P. O. Box 1663
Los Alamos, NM 87545

Characterization requirements for high gain laser fusion targets are severe. We are required to detect defects on the surfaces of opaque and transparent shells with an amplitude resolution of $\pm$ 5 nm and a spatial resolution of 1-10 μm. To achieve this we have developed a laser-illuminated phase-modulation interferometer. This instrument is based on a photoelastic polarization modulation technique which allows one to convert phase information into an intensity modulation which can be easily and sensitively measured using ac signal processing techniques. This interferometer has detected path length changes as small as 1 nm and the required spatial resolution is assured by using a microscope objective to focus the probe laser beam down to a small (~ 1 μm) spot on the surface of a microballoon. The interferometer will soon be coupled to an LSI-11 controlled 4π sphere manipulator which will allow us to automatically inspect the entire surface area of a target sphere.

A PHASE MODULATION INTERFEROMETER FOR ICF TARGET CHARACTERIZATION

David E. Cooper
University of California
Los Alamos National Laboratory
P. O. Box 1663
Los Alamos, NM 87545

Character'zation requirements for high gain laser fusion targets are severe. We will soon be required to detect localized defects on the surfaces of opaque and transparent shells with an amplitude resolution of ± 5 nm and a spatial resolution of 1 to 10 microns. To achieve this a novel phase shifting interferometer has been proposed.(1) We have constructed a similar interferometer which uses a different modulation techn!que based on the photoelastic polarization modulator.(2,3) This interferometer can detect 5 nm path length changes with a spatial resolution of 1 to 10 microns and can examine opaque as well as transparent targets. It will soon be interfaced to an LSI-11 controlled 4π sphere manipulator(4) which will allow us to automatically inspect the entire surface area of the target sphere.

With conventional interferometry one can at best visually detect a shift in an interference pattern of one-tenth of a fringe. In a double pass instrument, such as a Michelson Interferometer, this corresponds to a path length change of one-twentieth of a wave or about 25 nm for visible light. This sensitivity to path length changes can be significantly increased by using phase modulation interferometry. In our interferometer a phase measurement is converted into an intensity

measurement by sinusoidally modulating the relative phase of the two arms of the interferometer. Introduction of a phase object, such as a microballoon, in one arm of the interferometer results in an intensity modulation at a specific frequency on the output beam. The modulation depth is simply related to the phase shift induced by the sample object and can be easily and sensitively measured using standard ac signal processing techniques. With this technique we have detected path length changes as small as 1.0 nm.

Since we are dealing with coherent, polarized light it is convenient to discuss the propagation through the interferometer in the language of the Jones calculus.[5] In this language electric fields are represented by column vectors, known as Maxwell columns, whose components are complex numbers representing the amplitude and phase of the field. The effect of every optical element in a system can be represented by a 2 x 2 matrix. Multiplication of the input field vector by the representative matrix gives the output field from the corresponding optical element. In this language the effect of the modulator is represented by the matrix,

$$\begin{bmatrix} 1 & 0 \\ 0 & e^{i\delta} \end{bmatrix}$$

where $\delta = A \sin\omega t$, A is the relative phase amplitude and ω is the 50 kHz fundamental longitudinal resonance of the modulator. Figure 1 illustrates the interferometer design. Spatially filtered and expanded light from a helium-neon laser (632.8 nm) is plane polarized at $+45^{o}$ by a

Glan-Thompson prism. Assuming unit intensity, the light incident on the modulator is represented by the column vector $\frac{1}{\sqrt{2}}\begin{bmatrix}1\\1\end{bmatrix}$

The light output from the modulator is therefore,

$$\frac{1}{\sqrt{2}}\begin{bmatrix}1 & 0\\ 0 & e^{i\delta}\end{bmatrix}\begin{bmatrix}1\\1\end{bmatrix} = \frac{1}{\sqrt{2}}\begin{bmatrix}1\\e^{i\delta}\end{bmatrix}$$

This resulting polarization-modulated light then encounters a polarizing cube beamsplitter which transmits the $\begin{bmatrix}1\\0\end{bmatrix}$ component and reflects the $\begin{bmatrix}0\\e^{i\delta}\end{bmatrix}$ component through 90^{o}. The transmitted component becomes circularly polarized after passing through a suitably oriented quarter-wave plate and is then focused to a small spot on the surface of a microballoon by a strain-free (0.4 N.A.) microscope objective. By changing the expansion ratio of the laser-beam expander the spot diameter can be varied from 1 to 10 microns. If the microballoon is metallic the beam is reflected at normal incidence back through the objective and waveplate. Since the light has passed through the wave-plate twice, its polarization state is again linear but now given by the Maxwell column $\begin{bmatrix}0\\1\end{bmatrix}$. For a transparent microballoon one simply inserts a double-sided removable mirror at the location shown and the beam is reflected back through the target, objective pair and wave-plate. This probe beam is then deflected through 90^{o} on its next encounter with the cube beamsplitter. The $\begin{bmatrix}0\\e^{i\delta}\end{bmatrix}$ component is also circularly polarized by a quarter-wave plate and then is retroreflected by a reference mirror a second time through the wave plate becoming $\begin{bmatrix}e^{i\delta}\\0\end{bmatrix}$ light. This reference

beam is undeflected during its next pass through the cube beamsplitter. The probe and reference beams now travel a common path until they encounter a second cube beamsplitter. The same process is repeated with the exception that the probe beam is now focused onto the center of curvature of the target sphere (or is simply retroreflected by the removable mirror if the target is transparent). The advantage of this is that as the sphere is rotated by the 4π manipulator a small ($\pm$ 1 μm) movement of the sphere along the beam axis will not change the total path length of the probe beam.[6] Otherwise, small translations of the target sphere would give rise to the same signal as a surface defect. The probe and reference beams are recombined by the beamsplitter and then pass through a Soleil-Babinet compensator and Glan-Thompson prism. The compensator introduces a relative phase shift between the probe and reference beams which is easily adjustable to an accuracy of 5 nm. The Glan-Thompson prism, oriented at + 45°, interferes the orthogonal probe and reference beams and the resulting light intensity is then detected with a photodiode. In our matrix representation, the beam coming out of the interferometer has an electric field given by $\frac{1}{\sqrt{2}} \begin{bmatrix} e^{i\phi} \\ e^{i\delta} \end{bmatrix}$ where ϕ represents the phase shift due to any path length difference between the probe and reference arms. The effect of the compensator and polarizer is then,

$$\frac{1}{2\sqrt{2}} \begin{bmatrix} 1 & 1 \\ i & 1 \end{bmatrix} \begin{bmatrix} e^{-ic_1} & 0 \\ 0 & e^{-ic_2} \end{bmatrix} \begin{bmatrix} e^{i\phi} \\ e^{i\delta} \end{bmatrix}$$

$$= \frac{1}{2\sqrt{2}} \begin{bmatrix} e^{i(\phi - c_1)} + e^{i(\delta - c_2)} \end{bmatrix} \begin{bmatrix} 1 \\ 1 \end{bmatrix}$$

The intensity falling on the photodiode is therefore,

$$I = \frac{1}{2}\left[1 + \cos(\phi-\epsilon-\delta)\right] \tag{1}$$

where $\epsilon = \epsilon_1 - \epsilon_2$ is the relative phase shift induced by the compensator. Expanding the cosine in equation (1) and using the series expansions in Bessel functions for $\cos(\delta)$ and $\sin(\delta)$ yields,

$$I = \frac{1}{2}\left\{1 + \cos(\phi-\epsilon)\left[J_0(A) + \sum_{1}^{\infty} 2J_{2n}(A)\cos(2n\omega t)\right] + \sin(\phi-\epsilon)\left[\sum_{0}^{\infty} 2J_{2n+1}(A)\sin(2n+1)\omega t\right]\right\} \tag{2}$$

In practice we detect the component in equation (2) that oscillates at the fundamental,

$$I(\omega) = J_1(A)\sin(\phi-\epsilon)\sin\omega t \tag{3}$$

Introduction of a phase shift $(\phi-\epsilon)$ between the probe and reference waves results in an intensity modulation at the fundamental oscillation frequency (50 kHz) of the photoelastic modulator. This signal is detected by a lock-in amplifier referenced to the modulator.

A picture of the actual interferometer is shown in Figure 2. To obtain excellent thermal stability for the interferometer, most of its structure was fabricated out of super-invar (thermal expansion coefficient $\leq 3.6 \times 10^{-7}$). Optical elements of the interferometer rest on

super-invar plates which are kinematically mounted to two 1-inch-diameter super-invar rods. These rods are mounted on a super-invar fork which is in turn kinematically mounted to the optical table. To reduce the effects of floor vibration, air currents and acoustic coupling, the optical table is mounted on vibration isolation legs and both the table and interferometer are enclosed in plexiglass cages. Thermal drift in the laboratory is typically $\pm$ 0.5^{o}C during any 8-hour period. The effects of this drift on the interferometer are minimized by using all super-invar construction in several of the mirror mounts as well as low expansion (Zerodur) substrates for all mirrors. The physical path lengths of the probe and reference arms must only be matched to better than 0.5 cm since (assuming uniform thermal expansion of the super-invar framework) for each cm of path difference a 1^{o}C temperature change will give rise to a 3.6 nm drift.

In an actual microballoon examination the target will be held in the interferometer by the target rotator tips of the 4π manipulator. To facilitate the precise positioning of the target within the interferometer a viewing optics system will be set up which provides two orthogonal views of the target. One of these views is obtained by making one of the common path mirrors partially transmitting as shown. After a target is loaded, the compensator will be adjusted to null out any 50 kHz signal due to a path difference between the probe and reference beams. The sphere will then be rotated throughout its 4π solid angle by the computer-controlled manipulator and any probe path length changes brought about by localized surface defects or asphericities will be detected as a

50 kHz signal by the lock-in amplifier. In this way a detailed surface map of the sphere will be obtained.

Figure 3 shows a block diagram of the proposed automated sphere mapping system based on an LSI-11 microcomputer. A FORTRAN program will issue the commond sequence necessary to rotate the sphere under examination while simultaneously monitoring the 50 kHz output of the lock-in amplifier. Examination times should typically be on the order of 5 minutes for a 500 micron diameter shell. After an inspection, the surface map of the sphere will be displayed on a graphics terminal and stored on magnetic disk. To facilitate comparision with other targets a hard copy of the surface map can be generated for the graphics display.

FIGURES

Figure 1. Phase Modulation Interferometer.

Figure 2. The Phase Modulation Interferometer on Super-Invar Framework

Figure 3. Automated Sphere Mapping System.

REFERENCES

(1) J. A. Monjes, B. W. Weinstein, D. L. Willenborg, Reflection/Transmission Phase Shift Interferometer and Viewing Optics, UCRL-85281.

(2) S. M. Jasperson and S. E. Schnatterly, Rev. Sci. Inst. 40, 761-767 (1969).

(3) J. C. Kemp, J. Opt. Soc. Am. 59, No. 8 (1969).

(4) J. A. Monjes, B. W. Weinstein, D. L. Willenborg and A. L. Richmond, Microsphere Rotator, UCRL-83375.

(5) A. Gerrard and J. M. Burch, Introduction to Matrix Methods in Optics, John Wiley and Sons (1975) pp 207-221.

(6) Laser Program Annual Report - 1979, Lawrence Livermore Laboratory, Livermore, California, UCRL-50021-79 (1981), pp. 4-42 to 4-45.

(7) J. W. Berthold, S.F. Jacobs and M. A. Norton, Metrologia 13, 9-16 (1977).

PHASE MODULATION INTERFEROMETER

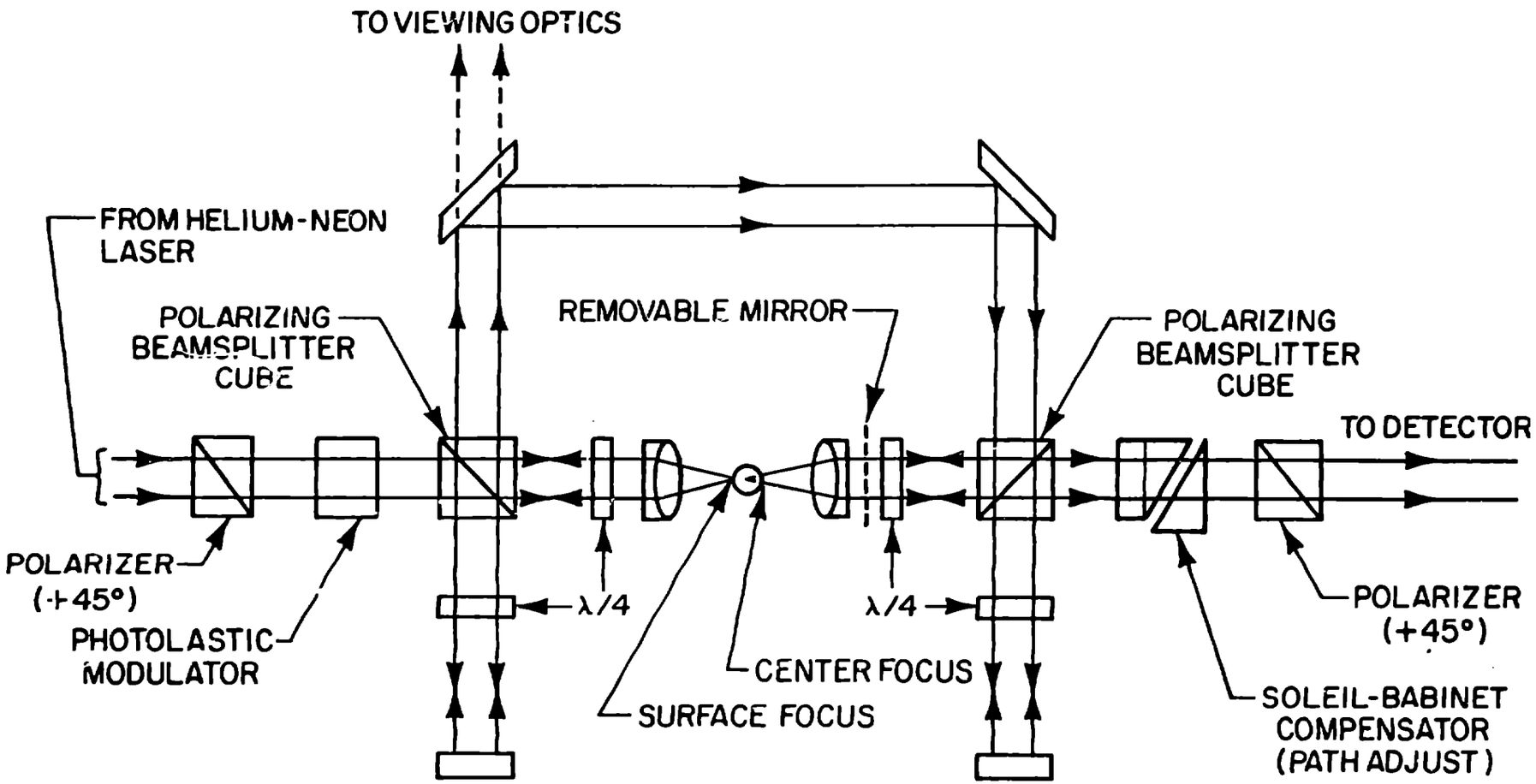

Figure 1

LOS ALAMOS NATIONAL LABORATOR
LOS ALAMOS, NEW MEXICO

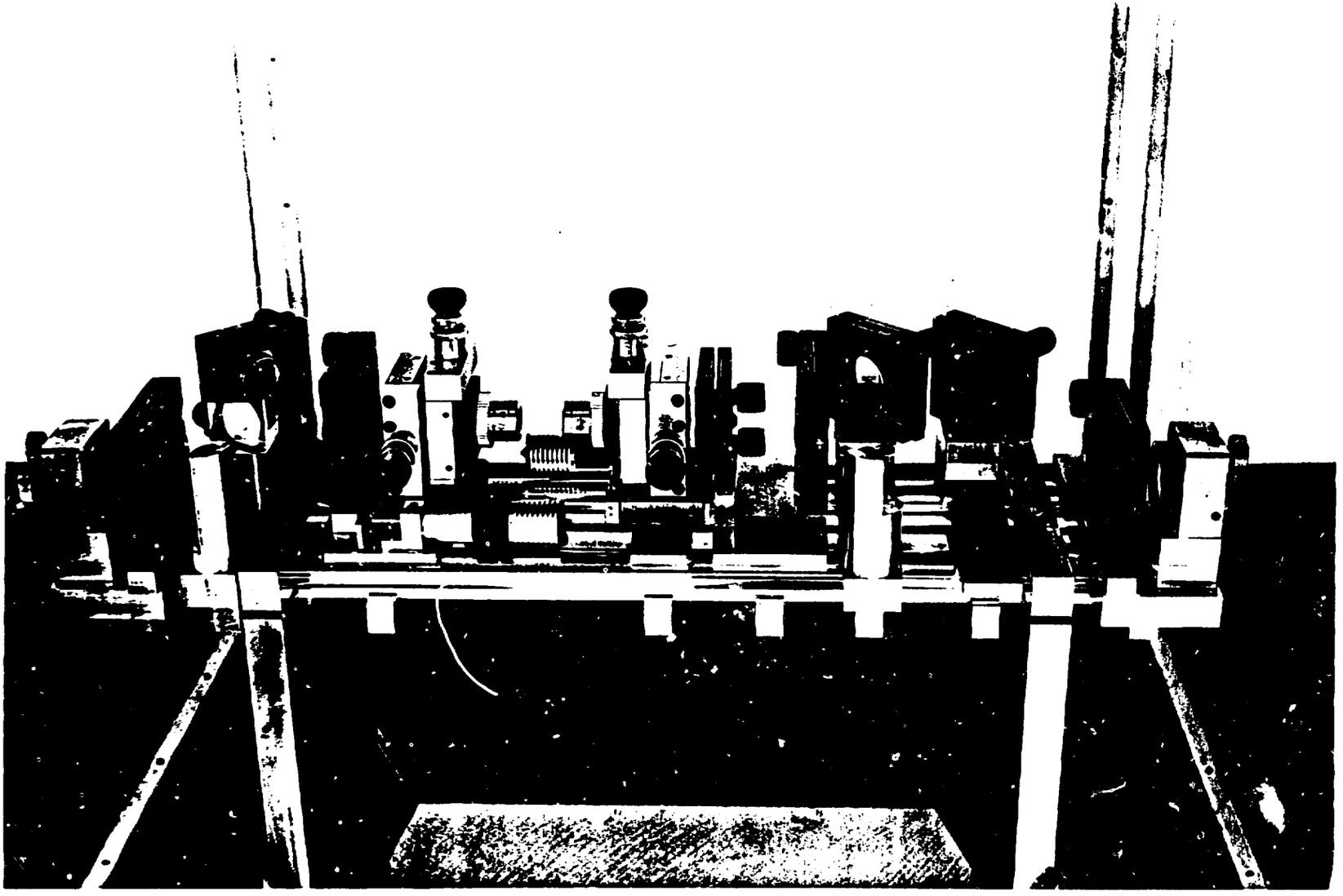

AUTOMATED SPHERE MAPPING SYSTEM

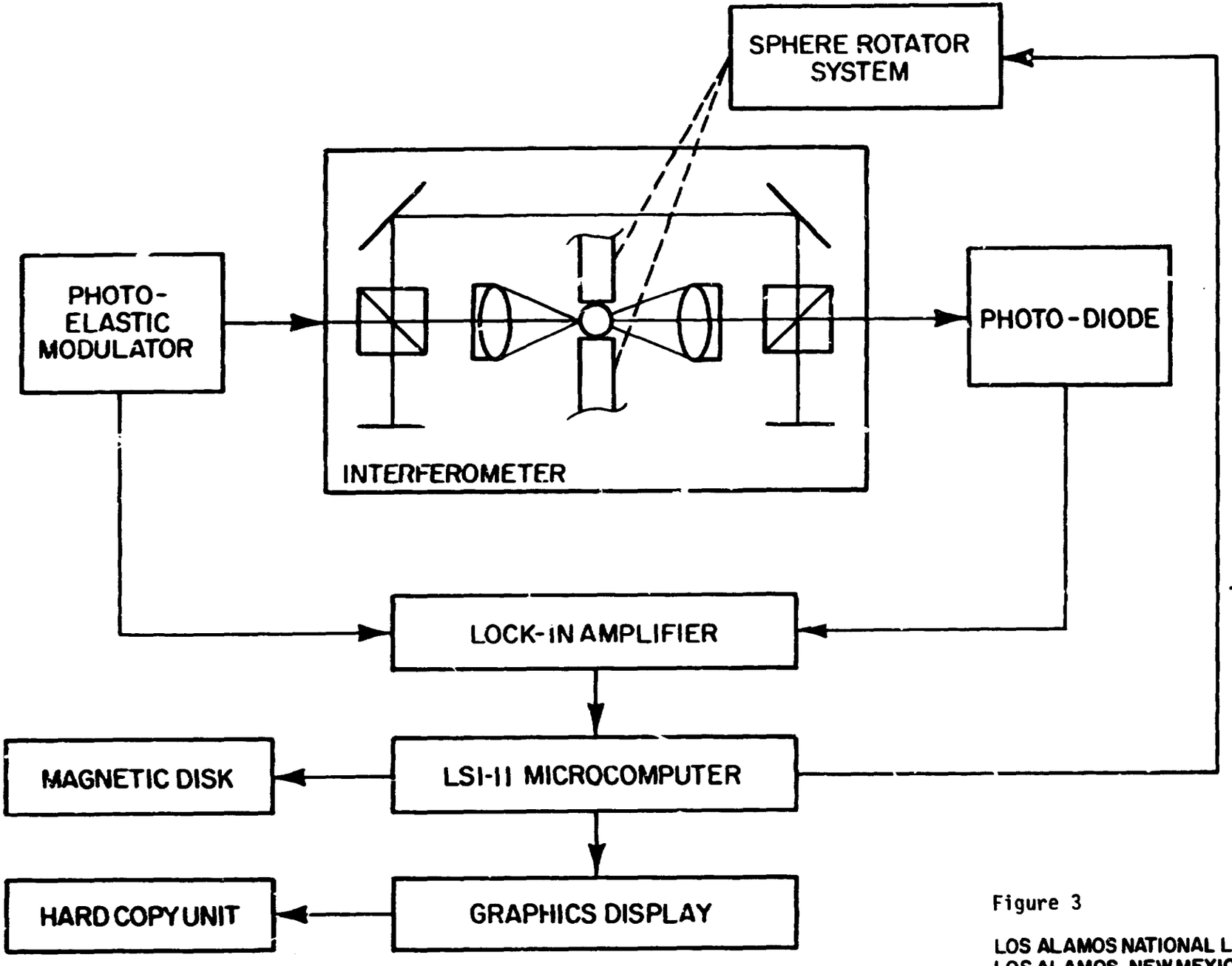

Figure 3

LOS ALAMOS NATIONAL LABORATO
LOS ALAMOS, NEW MEXICO